Available online at www.sciencedirect.com

ScienceDirect

Procedia CIRP 123 (2024) 143–148

www.elsevier.com/locate/procedia

7th CIRP Conference on Surface Integrity

Prediction of Surface Profile in CFRP Machining through Phenomenological Analysis and inverse Continuous Wavelet Transformation

Alexander Brouschkin[a]*, Lars Köttner, Wolfgang Hintze[a], Jan Dege[a],

[a] *Institute of Production Management and Technology, Hamburg University of Technology, Denickestr. 17, 21073 Hamburg*

* Corresponding author. Tel.: +49 40 428 78 3264; *E-mail address:* alexander.brouschkin@tuhh.de

Abstract

Carbon fibre-reinforced polymer (CFRP) is favored for its high strength to weight ratio, outstanding direction dependent mechanical properties and the high potential for load adapted design. However, machining unidirectional CFRP is challenging due to its anisotropic behavior, resulting in variable surface quality under identical machining parameters with different fibre orientations.

Recently, a universal, process-independent model describing the engagement conditions in oblique cutting of unidirectional CFRPs has been developed, introducing the spatial fibre cutting angle θ_0 and the spatial engagement angle ϕ_0. Milling and drilling are mostly used for machining CFRP. Since the engagement conditions are rather complex, first analogy experiments are conducted in turning with variation of the setting and inclination angles.

In this study, continuous surface profiles were recorded as a function of the spatial fibre cutting angle. Phenomenological and continuous wavelet analyses can be used to describe the surface profiles as a function of the spatial engagement conditions and to accurately predict them and the surface roughness using an inverse wavelet transformation. Experimental investigations with a side milling process of CFRP validate the prediction approach and show a good agreement between the experimental and predicted surface profiles.

*Keywords:*carbon fibre reinforced plastics; carbon fibre reinforced polymers ,cutting; turning; sawing; spatial engagement conditions; surface roughness

1. Introduction

Carbon fibre-reinforced polymer (CFRP) is favored for its high strength to weight ratio, outstanding direction dependent mechanical properties and the high potential for load adapted design. However, machining unidirectional CFRP is challenging due to its anisotropic behavior, resulting in variable surface quality under identical machining parameters with different fibre orientations.

CFRP consists of two main components: carbon fibres and a polymer matrix. The fibre is the essential component responsible for the outstanding mechanical properties of the composite, while the matrix maintains the fibres in the necessary shape, provides support against transverse loads and protection against environmental influences. Thermoset or thermoplastic polymers can be used for the matrix.

Machining CFRP yields in high surface roughness with a high standard deviation [1] and a fluctuating surface quality depending on the fibre orientation. The optimum surface roughness was obtained under a $\theta = 135\,°$ fibre orientation, whereas the worst was obtained at $\theta = 45\,°$. [2]. Fibres shape the manufactured surface, as fibre orientation significantly influences surface roughness [3]. When processing CFRP, various failure modes of the composite could be observed: fibre fracture and inter-fibre fracture. [3, 4, 5]. The fibre can characteristically fail due to tensile stress, compressive stress, or a combination of both in a bending failure [3, 5]. A shear failure of the fibre usually does not occur, as an inter-fibre

2212-8271
10.1016/j.procir.2024.05.027

fracture occurs even at relatively low shear loads [4]. An inter-fibre fracture refers to the separation of the matrix from the fibre, resulting in a long crack along the fibre direction and causing a stepped surface during the processing of CFRP [3]. This phenomenon occurs with specific fibre orientations and low loads and is characterized by the debonding of the fibre and matrix [3].

Nomenclature

CFRP	Carbon reinforced polymer
cwt	continuous wavelet transformation
d_f	fibre diameter [µm]
v_c	cutting velocity [m/min]
v_f	feed velocity [mm/min]
h	undeformed chip thickness [mm]
f	feed rate [mm/min]
κ_r	setting angle [°]
ρ	tilt angle [°]
λ_s	inclination angle [°]
α_o	clearance angle [°]
γ_o	rake angle [°]
r_β	cutting edge radius [µm]
d_t	diameter of the cutting tool [mm]
h_t	height of the side milling cutter above the CFRP laminate [mm]
$\overrightarrow{e_{\|\|}}, \overrightarrow{e_{\perp 1}}, \overrightarrow{e_{\perp 2}}$	coordinate system of the CFRP laminate
$\overrightarrow{e_r}, \overrightarrow{e_s}, \overrightarrow{e_o}$	coordinate system of the cutting tool
θ	fibre cutting angele [°]
χ, ξ	reference angles [°]
θ_0	spatial fibre cutting angle [°]
ϕ_0	spatial fibre engagement angle [°]
l_n	total measurement length [mm]
v_m	measuring speed [mm/s]
λ_c	cut-off wavelength [mm]
Ra	linear arithmetic roughness [µm]
Rz	mean maximum peak to valley height in a sampling length [µm]
Rt	maximum peak to valley height [µm]
λ	profile wavelength [µm]
δ	profile wave depth [µm]

The influence of fibre fracture on the surface roughness can be estimated to values below the fibre diameter d_f = 6 - 7 µm. While the influence of inter-fibre fracture is significantly higher due to the detachment of entire fibre bundles. According to Puck, inter-fibre fracture predominantly occurs at a fibre orientation of θ = 50 – 55 °[6]. During the processing of CFRP, inter-fibre failures have been observed, at θ = 45 ° [4] and within the range of θ = 25 °- 75 °, as well as at θ = 150 ° [3]. This is characterized by a stepped surface, the widths and depths of which depend on the fibre orientation. Wang et al. reported widths of up to 800 µm and depths of up to 30 µm [3]. Furthermore, the shape of the stepped surface depends on the cutting speed v_c [7, 3] and feed rate f [3]. On this basis, Gara et al. developed a theoretical model for predicting the arithmetic roughness Ra for up and down milling based on cutting speed v_c and feed rate f, without considering fibre orientation [8]. Song et al. predicted the surface roughness in high-speed dry milling of CFRP for a fibre orientation of θ = 90 ° [9].

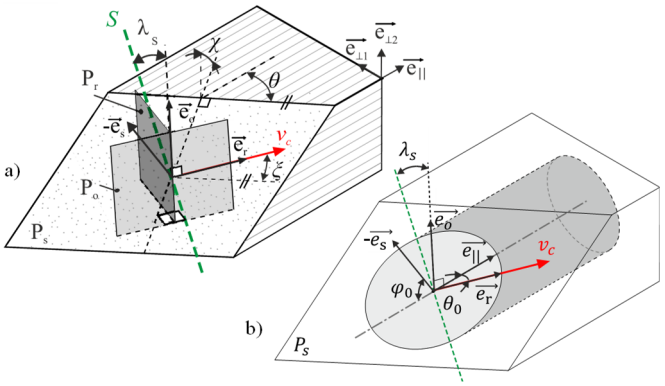

Figure 1: a) Workpiece coordinate system and the tool coordinate system with the reference angles, b) spatial engagement angles

To characterize the roughness of composite materials, Ra, Rz, Rt, and Rk are commonly used. Rk specifically characterizes process roughness, disregarding anatomical roughness which is influenced by the workpiece material and therefore by fibre orientation. Ra, Rz, and Rt include the behavior of anatomical roughness. [10]

Recently, a universal, process-independent model describing the engagement conditions in oblique cutting of unidirectional CFRPs has been developed, introducing the spatial fibre cutting angle θ_0 and the spatial engagement angle φ_0 [11, 12]. Thus, an opportunity was created to consider roughness independently of the machining process.

In this study, a process-independent model for predicting the roughness profile in the cutting direction is generated based on measurement data. To create the database, transversal internal turning was chosen as analogy process, due to the simple engagement conditions. Surface profiles of unidirectional CFRP are experimentally generated and recorded depending on the fibre cutting angle θ and the setting angle κ_r. Thereby the cutting velocity v_c and the undeformed chip thickness h is hold constant. Using continuous wavelet transformation, the characteristic widths and depths of the resulting stepped surface for different fibre cutting angles are determined. When transferred to the process-independent description of the engagement conditions, this data is linearly interpolated. Using inverse wavelet transformation, a profile can be predicted for arbitrary engagement conditions. The process-independent model is validated in the process of side-milling. Predicting the profile allows for the determination of roughness parameters such as Ra, Rz, and Rt with the profile.

2. Process-independent description of fibre-engagement conditions

Hintze et al. developed a process-independent description of the spatial engagement conditions during the oblique cut of CFRP with reference angles, in which they applied a transformation of the workpiece coordinate system $\{\overrightarrow{e_{||}}, \overrightarrow{e_{\perp 1}}, \overrightarrow{e_{\perp 2}}\}$ into the tool coordinate system $\{\overrightarrow{e_r}, \overrightarrow{e_s}, \overrightarrow{e_o}\}$ (Figure 1) [11, 12]. With the reference angles θ, χ, ξ and the inclination angle λ_s any cutting process can be described. Taking into account the orthotropy of the material, Hintze et al. [11] introduce the spatial engagement angles, which describe

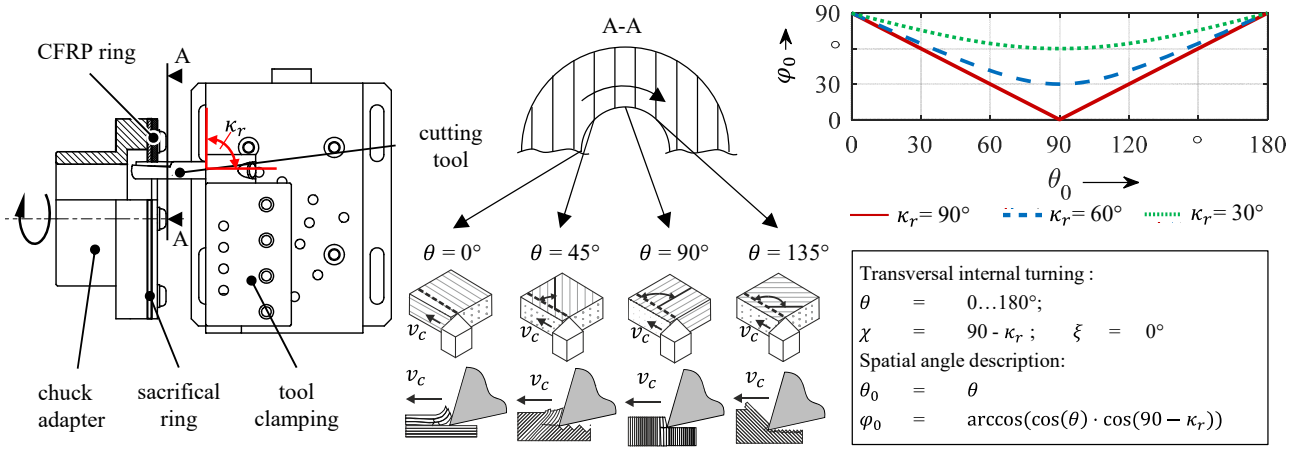

Figure 2: Experimental set up: Turning. Reference angles and spatial angles for transversal internal turning

the spatial angles between the vectors $\overrightarrow{e_s}$ and $\overrightarrow{e_{||}}$ for the spatial fibre cutting angle θ_0 and between the vectors $\overrightarrow{e_r}$ and $\overrightarrow{e_{||}}$ for the spatial engagement angle φ_0, as shown in Figure 1 a). With the equations (1-3) θ_0 and φ_0 can be calculated.

$$\begin{pmatrix} \overrightarrow{e_{||}} \\ \overrightarrow{e_{\perp 1}} \\ \overrightarrow{e_{\perp 2}} \end{pmatrix} = \begin{bmatrix} \cos\theta & \sin\theta & 0 \\ -\sin\theta & \cos\theta & 0 \\ 0 & 0 & 1 \end{bmatrix} \cdot \begin{bmatrix} 1 & 0 & 0 \\ 0 & \cos\chi & \sin\chi \\ 0 & -\sin\chi & \cos\chi \end{bmatrix} \cdot \begin{bmatrix} \cos\xi & 0 & -\sin\xi \\ 0 & 1 & 0 \\ \sin\xi & 0 & \cos\xi \end{bmatrix} \cdot \begin{pmatrix} \overrightarrow{e_r} \\ \overrightarrow{e_s} \\ \overrightarrow{e_o} \end{pmatrix} \quad (1)$$

$$\cos(\theta_0) = \langle e_r, e_{||} \rangle \quad (2)$$

$$\cos(\varphi_0) = \langle e_r, e_s \rangle \quad (3)$$

3. Experimental setup

3.1. Transversal internal turning set up

The experiments are carried out in transverse internal turning. A cemented carbide cutting tool (grade CERATIZIT CTS12D) with a Oerlikon BALDIA® COMPOSITE DC diamond coating (thickness of 12+3 µm), a clearance angle $\alpha_o = 6$ °, a rake angle $\gamma_o = 10$ ° and a cutting-edge radius $r_\beta = 20$ µm is used as cutting tool and a CFRP ring with a thickness of d = 4 mm made out of unidirectional CFRP (HexPly 6376, Prepreg, HTS 12k) is turned outwards through a previously made bore hole (D = 70 mm). To avoid delamination and deformation of the CFRP ring, a sacrificial ring out of aluminum (thickness d = 2 mm) is clamped between the chuck adapter and the CFRP ring. This supports the CFRP ring at low κ_r and thus prevents delamination.

To realize different spatial engagement conditions, the setting angle κ_r and the fibre cutting angle are varied. θ changes from 0 ° to 180 ° due to the rotation of the workpiece twice per revolution as shown in Figure 2. The setting angle κ_r is varied in three steps $\kappa_r = 90$ °, $\kappa_r = 60$ ° and $\kappa_r = 30$ ° to cover the θ_0-φ_0-plane evenly. As further influencing factors the inclination angle λ_s is held constant at $\lambda_s = 15$ ° and the undeformed chip thickness at h = 40 µm resulting in different feed rates for different setting angles κ_r.

In order to eliminate the influence of the chip thickness on the roughness, the cutting edge must be withdrawn from the cut in a maximum time corresponding to half a revolution, so that one half of the bore surface is not machined with a lower chip thickness that occurs when the cutting edge is withdrawn from the cut. For this a max. reverse feed of $v_f = 5000$ mm/min the cutting velocity v_c is set to $v_c = 50$ m/min. No indication of the withdrawal of the cutting edge could be detected on the cut surface. Assuming that one half of the ring has lower h, the whole surface was measured and only the half with the highest profile peaks were used.

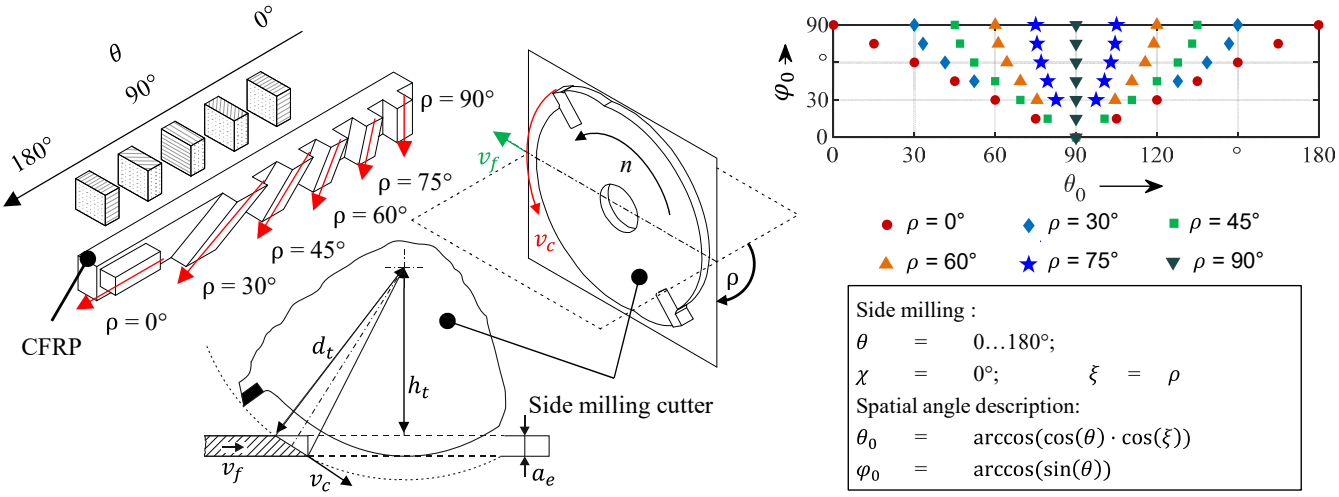

Figure 3: Experimental set up: side milling. Reference angles and spatial angles for side milling.

3.2. Side milling set up

The validation experiments are carried out in side milling, which is applied as a circular sawing process. A CERATIZIT SF-D100-SX6-Z4-AD22-DC with a milling diameter of d_t = 100 mm with one cemented carbide insert (grade: CERATIZIT CTS18D) with Oerlikon BALDIA® COMPOSITE DC diamond coating (thickness of 12+3 µm) with a clearance angle α_o = 6 °, a rake angle γ_o = 10 ° and an inclination angle λ_s = 15 ° is used as cutting tool and a CFRP plate with the thickness of a_e = 6 mm made of unidirectional CFRP-specimen (HexPly 6376, Prepreg, HTS 12k) is machined. To prevent imbalance, a non-cutting insert is placed opposite to the cutting insert. To realize different spatial engagement conditions, the tilt angle ρ and the fibre cutting angle θ are varied (Table 1). These are chosen to evenly cover the θ_0-φ_0-plane. Furthermore, the height of the side milling cutter above the CFRP laminate is set to h_t = 0 mm (Figure 3), so the rotation axis of tilt angle ρ is in the upward laminate plane. As further influencing factors the cutting velocity is held constant to the turning set up by v_c = 50 m/min resulting in a rotational speed of n =160 rpm and an undeformed chip thickness of h = 40 µm resulting in a feed rate of v_f = 6.4 mm/min. Due to the use of plunge slotting, kinematic roughness can be neglected. Furthermore, to avoid the appearance of lower h in the processes the tool is withdrawn from the cut with a maximum feed velocity of 4000 mm/min.

Table 1: Fibre cutting angle θ and tool tilt angle ρ for the side milling experiments

Fibre cutting angle θ	Tool tilt angle ρ
0°, 15°, 30°, 45°, 60°, 75°, 90°, 105°, 120°, 135°, 150°, 165°, 180°	0°
0°, 15°, 30°, 45°, 135°, 150°, 165°, 180°	30°
0°, 15°, 30°, 45°, 60°, 75°, 90°, 105°, 120°, 135°, 150°, 165°, 180°	45°
0°, 15°, 30°, 45°, 60°, 120°, 135°, 150°, 165°, 180°	60°
0°, 15°, 30°, 45°, 60°, 120°, 135°, 150°, 165°, 180	75°
0°, 15°, 30°, 45°, 60°, 75°, 90	90°

3.3. Roughness Measurements

A tactile, stylus type perthometer is used to measure the surface profile. Here, the profile is measured parallel to the cutting speed direction. To perform this measurement within the turning setup, the CFRP-ring is clamped into a CNC axis using a chuck adapter and rotated at a measurement speed of v_m = 0.5 mm/s, with the measuring stylus held stationary. To determine the roughness parameters the evaluation parameters are l_n = 5.6 mm and λ_c = 0.8 mm, as suggested in DIN EN ISO 21920. As roughness parameter Rz was chosen because it introduces stochasticity compared to Rt and highlights the height of the steps compared to Ra. For the representation of the results in the θ_0-φ_0-plane, the average values of single measurements at each θ_0-φ_0-combination is interpolated linearly. R^2 indicates accordingly the deviation of the single measurements at each measured θ_0-φ_0-combination.

4. Prediction model

As the primary aspect of the investigation was the localization and characterization of the profile waves regardless of discretization, the continuous wavelet transformation (cwt) was used. To acquire the cwt the analytical Morse wavelet is used, with a symmetry parameter, γ = 3, and a time-bandwidth product set to 60. The determination of the minimum and maximum scales is automated, relying on the energy spread of the wavelet in frequency and time. For constructing the prediction model, four surface profiles per turning setting angle are transformed into the wavelet domain. Since the profiles have varying lengths, data is sampled in 1 ° increments, corresponding to l = 0.5 mm per fibre cutting angle θ, for the model. This transformation yields profile wavelengths ranging from λ = 1 µm to λ = 30 mm. The data, averaged over four measurements, is then converted into the θ_0-φ_0- description. Subsequently, for each profile wavelength from λ = 50 µm to λ = 30 mm, amplitudes and phases in the wavelet domain are interpolated. To limit the storage requirements, profile wavelengths λ < 50 µm were disregarded due to their low amplitude.

To retrieve the model, the evolution of θ_0 and φ_0 is modelled for the corresponding process parameters. The amplitude and phase are extracted for each profile wavelength, and the profile is assembled in the wavelet domain. Due to the interpolation in the wavelet domain, the inverse wavelet transformation results in a halved amplitude and doubled profile wavelength. The amplitude δ before the inverse wavelet transformation is doubled. To correct the profile

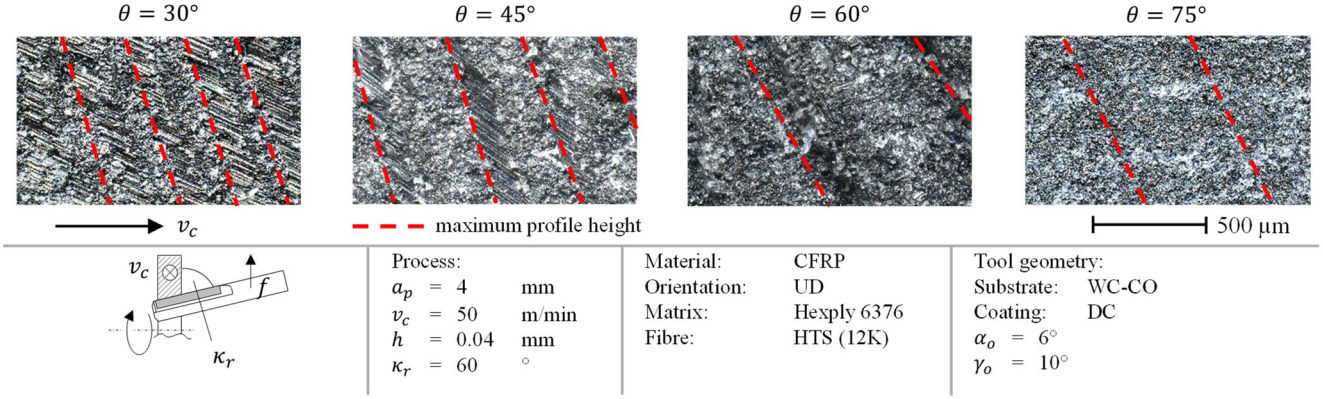

Figure 4: Machined surface at different θ for constant tool settings of κ_r = 60°

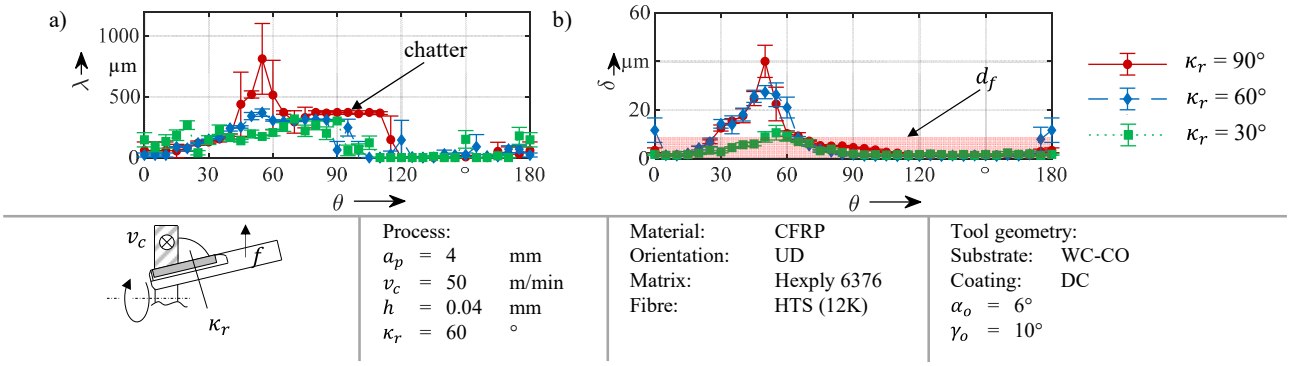

Figure 5: a) profile wavelength λ and b) profile height δ as a function of θ and κ_r.

wavelength λ, the profile is stacked twice and inverse-transformed at half the resolution. Subsequently, roughness parameters can be determined from the profile.

5. Results

5.1. Transversal internal turning

Figure 4 depicts the resulting stepped surface within the fibre cutting angle range of 15° < θ < 75 °. A regular formation of the steps is visible. In Figure 5a, the step width λ is plotted as a function of the fibre cutting angle θ which is derived of the cwt of the surface profile. Across all setting angles, the surface exhibits an increased step width, reaching up to λ = 900 µm, in the fibre cutting angle range of 15° < θ < 75°. Notably, a plateau is observed at λ = 340 µm within the fibre cutting angle range of 75° < θ < 115 ° for κ_r = 90 °. This was attributed to tool chatter at κ_r = 90°. The profile depth increases with the width, reaching a maximum of δ = 40 µm at θ = 50 ° (Figure 5b). The micrograph (Figure 6) reveals irregularities in the step pattern that span multiple steps. These occur independently of the machining process and are likely attributed to local variations in fibre volume content.

5.2. Predicting the surface profile

Figure 6 shows the measured and predicted profile of the side milling machining at θ = 30 ° and ρ = 45 °. The comparison between the measured and the simulated surface profile shows a high accordance. Nevertheless, the profile height is predicted slightly higher than the actual measurement. A slight local deviation in the profile wavelength can be attributed to the random nature of fracture propagation. This may have been caused by local variations in fibre volume content or undulations in the fibres. In Figure 7a the roughness Rz is shown for side milling. The highest Rz values are measured for φ = 45 °and decreases away from φ_0 = 45 °. For all θ_0 < 90 ° the roughness Rz is of the same magnitude as the fibre diameter d_f = 7 µm. Furthermore, the standard deviation of the measurements is lower than 10 µm (Figure 7c). The prediction model results in a maximum of Rz in the range 30° < θ_0 < 75 ° and 30° < φ_0 < 15 °. For other engagement conditions, a low roughness value of Rz = 6 – 10 µm is observed which in the range of the fibre diameter d_f = 7 µm (Figure 7b). Comparing the roughness (Rz) for side milling with the prediction model reveals that the predicted values differ by up to 10 µm from the mean values of the measurements. (Figure 7d) However, in three measurements, the difference between the model and the measurement is much higher. In the first area for φ_0 = 45 °, θ_0 = 45 ° a deviation of the prediction model is higher than ΔRz = 15 µm which can be explained by reduced tool chatter in side milling than in turning. However, the second area for φ_0 = 45 °, θ_0 = 72 ° and θ_0 = 82.7 ° the deviation is up to $|\Delta Rz|$ = 30 µm. This could indicate a significant difference of the two machining processes.

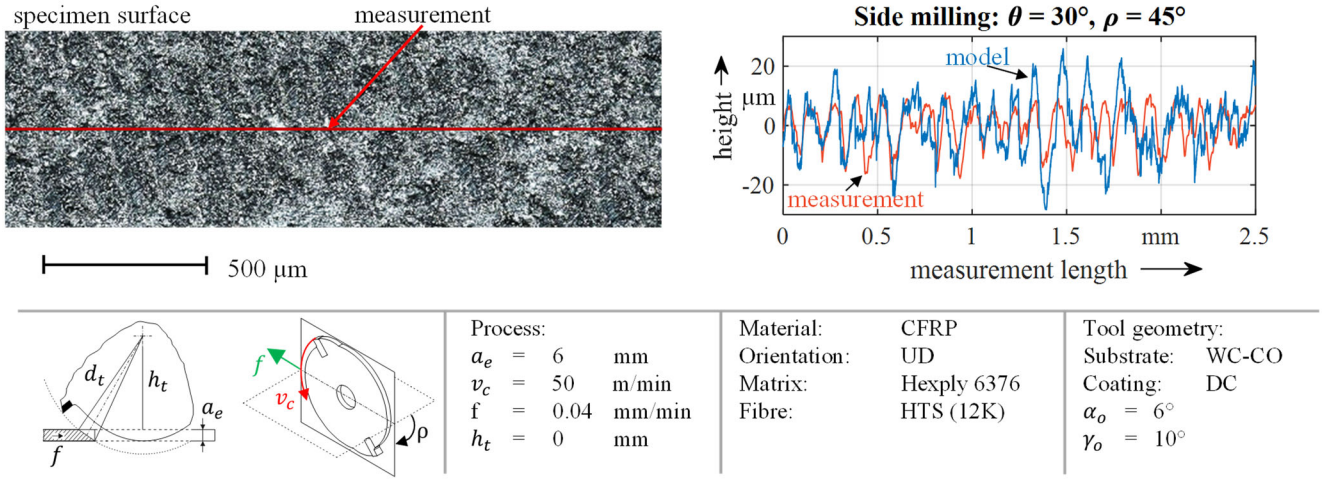

Figure 6: Comparison of the measured and predicted surface profile at θ = 30° and ρ = 45°

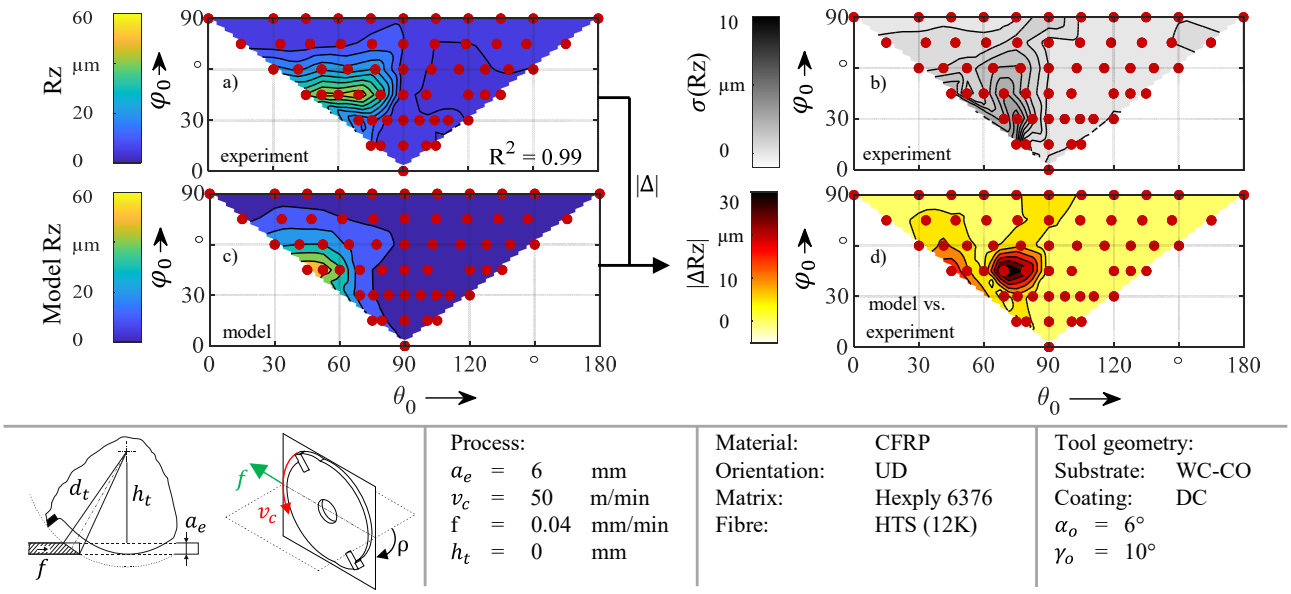

Figure 7:In the θ_0-φ_0-plane a) Roughness Rz in side milling CFRP, b) standard deviation of Rz in side milling CFRP, c) Roughness Rz of the prediction model, d) Difference between the prediction model and the measurements.

6. Summary and Outlook

With the spatial description of the engagement conditions during machining of CFRP the following results can be stated regarding the surface roughness and the prediction model.

- The developed prediction model can accurately forecast the profile wavelength, with the wave height being slightly overpredicted in comparison to the actual measurements.
- Process-independent predictions are fundamentally feasible, with reference to the spatial description of the engagement conditions. Demonstrated in this work, by the prediction of the surface profile of CFRP machined with side milling using data derived from turning operations.
- The developed prediction model anticipates surface roughness within the θ_0-φ_0-plane well, except for three measurements that deviate by more than $|\Delta Rz| = 10\mu m$.
- In future it is planned to enhance the model in order to predict roughness in other machining processes based on data derived from turning analogy experiments, including the combination of material roughness and kinematic roughness in peripheral milling.

Acknowledgements

The authors gratefully acknowledge the financial support of the German Research Foundation, Deutsche Forschungsgemeinschaft (DFG) within the research project HI 843/13-1, project number 457264004.

References

[1] Pecat O., Brinksmeier E., Low Damage Drilling of CFRP/Titanium Compound Materials for Fastening, Procedia CIRP 13 (2014) 1 – 7, 2nd CIRP 2nd CIRP Conference on Surface Integrity (CSI), doi: 10.1016/j.procir.2014.04.001

[2] Kumar D., Gururaja S., Machining damage ans surface integrity evaluation during milling of UD-CFRP laminates: Dry vs. cryogenic, Composite Structures (2020) 112504, http://dx.doi.org/10.1016/j.compstruct.2020.112504

[3] Wang C., Liu G., An Q., Chen M., Occurence and formation mechanism of surface cavity defects during orthogonal milling of CFRP laminates, Composites Part B 109 (2017) 10e22, http://dx.doi.org/10.1016/j.compositesb.2016.10.015

[4] Calzada K.A., Kapoor S.G., DeVor R.E., Samuel J.,Srivastava K., Modeling and interpretation of fiber orientation-based failure mechanisms in machining of carbon fiber-reinforced polymer composites, Journal of Manufacturing Processes 14 (2012) 141–149, doi:10.1016/j.jmapro.2011.09.005

[5] Rummenhöller S, Werkstofforientierte Prozessauslegung für das Fräsenkohlenstoffaserverstärkter Kunststoffe, Dissertation (1996), Shaker, Aachen

[6] Puck A., Schürmann H., Failure analysis of FRP laminates by means of physically based phenomenolical models, Composites Science and Technology Volume 62, Issues 12–13, September–October 2002, Pages 1633-1662, https://doi.org/10.1016/S0266-3538(01)00208-1

[7] Nguyen-Dinh N., Zitoune R., Bouvet C., Leroux S., Surface integrity while trimming of composite structures: X-ray tomography analysis, Composite Structures 210 (2019) 735–746, https://doi.org/10.1016/j.compstruct.2018.12.006

[8] Gara s., Tsoumarev O., Prediction of surface roughness in slotting of CFRP, Measurement 91 (2016) 414–420 (2016), http://dx.doi.org/10.1016/j.measurement.2016.05.016

[9] Song Y., Cao H., Wang Q., Zhang J., Yan C., Surface roughness prediction model in high-speed dry milling CFRP considering carbon fiber distribution, Composites Part B 245 (2022) 110230, https://doi.org/10.1016/j.compositesb.2022.110230

[10] Gurau L., Irle M., Surface Roughness Evaluation Methods for Wood Products: a Review, Curr Forestry Rep (2017) 3:119–131, DOI 10.1007/s40725-017-0053-4

[11] Hintze W., CFK-Bearbeitung- Trenntechnologien für Faserverbundkunststoffe und den hybriden Leichtbau., Springer-Verlag, 2021, ISBN 978-3-662-63265-9, https://doi.org/10.1007/978-3-662-63265-9

[12] Hintze, W.; Brouschkin, A.; Köttner, L.; Bluehm, M.,Model Based Prediction of Force and Roughness Extrema Inherent in Machining of Fibre Reinforced Plastics Using Data Merging, Proceedings of the 12th Congress of the German Academic Association for Production Technology (WGP), University of Stuttgart, October 2022, Springer Verlag Berlin, 2022, DOI: 10.1007/978-3-031-18318-8_5